

# X-Ray Diffraction Study on the Structure of Molten $\text{Mg}_x\text{Zn}_{(100-x)}$ -Alloys

E. Bühler, P. Lamparter, and S. Steeb

Max-Planck-Institut für Metallforschung, Institut für Werkstoffwissenschaften, Stuttgart

Z. Naturforsch. **42a**, 507–510 (1987); received January 31, 1987

By means of X-ray diffraction in transmission the molten  $\text{Mg}_x\text{Zn}_{(100-x)}$ -alloys ( $x = 0, 8, 15, 30, 40, 50, 60, 70, 73, 80, 90, 100$ ) were investigated and the total structure factor  $S(Q)$ , the total pair correlation function, the number of nearest neighbours as well as the atomic distances were evaluated. For  $30 \leq x \leq 80$  a premaximum in  $S(Q)$  was observed which is caused by chemical short range order. The comparison of the premaximum of the  $\text{Mg}_{70}\text{Zn}_{30}$ -melt with that of the corresponding amorphous alloy shows that within the melt the chemical short range order amounts to about 40% of that of the amorphous alloy.

## Introduction

Premaxima in the structure factor were observed with the Mg-base alloys Mg–Ag [1], Mg–Sn [2], Mg–Cu [3], and  $\text{Mg}_{70}\text{Zn}_{30}$  [4]. The occurrence of premaxima is caused by chemical short range order (CSRO). In the present work the concentration dependence of the CSRO in molten  $\text{Mg}_x\text{Zn}_{(100-x)}$ -alloys is investigated.

## Experimental

### 1. Specimen Preparation

The chemical purity of Mg as well as of Zn was 99.9%. The starting ingot was prepared by induction melting in argon-atmosphere. The specimen thickness was 0.03 mm (Zn) up to 1.3 mm (Mg).

### 2. Apparatus

The X-ray diffraction experiments were done using a diffractometer D 500 (Siemens, Karlsruhe) in transmission. Always two runs were necessary with each specimen since the method of balanced filters was applied to extract the scattering signal corresponding to the Mo-K $\alpha$ -radiation. The melts were kept between beryllium windows within a steel frame. The angle region was  $3^\circ \leq 2\theta \leq 101^\circ$  cor-

responding to  $0.46 \text{ \AA}^{-1} \leq Q \leq 13.7 \text{ \AA}^{-1}$  with Mo-K $\alpha$ -radiation, where

$$\begin{aligned} Q &= 4\pi(\sin\theta)/\lambda, \\ 2\theta &= \text{scattering angle}, \\ \lambda &= \text{wavelength}. \end{aligned} \quad (1)$$

## Results and Discussion

### 1. Total Structure Factors

Figure 1 shows the Faber Ziman total structure factors  $S_t^{FZ}(Q)$  of molten  $\text{Mg}_x\text{Zn}_{(100-x)}$ -alloys obtained by X-ray diffraction. These functions were derived from the measured data by correction for polarization [5], absorption [6], and fluorescence. The normalization was done according to [7], and then the incoherently scattered intensity [8] was subtracted. The temperature  $T$  of the melts was always by  $40^\circ\text{C}$  higher than the corresponding liquidus temperature  $T_L$ . The curves as shown in Fig. 1 are smoothed in the region  $Q \geq 3.5 \text{ \AA}^{-1}$  using a cubic splinefit algorithm.

We observe a shift of the maxima of  $S(Q)$  to larger  $Q$ -values with increasing Zn-concentration. On the left hand side of the main peak we observe for  $30 \leq x \leq 80$  a prepeak which is most pronounced for the  $\text{Mg}_{70}\text{Zn}_{30}$  melt. The second peak for  $x = 70$  and 73 shows a slight shoulder on its right hand side. The comparison with the structure factors obtained with amorphous  $\text{Mg}_{70}\text{Zn}_{30}$  as well as  $\text{Mg}_{72}\text{Zn}_{28}$  shows a more pronounced shoulder in the two latter cases [9, 10].

Reprint requests to Prof. Dr. S. Steeb, MPI für Metallforschung, Institut für Werkstoffwissenschaften, Seestraße 92, 7000 Stuttgart 1.

0932-0784 / 87 / 0500-0507 \$ 01.30/0. – Please order a reprint rather than making your own copy.



Dieses Werk wurde im Jahr 2013 vom Verlag Zeitschrift für Naturforschung in Zusammenarbeit mit der Max-Planck-Gesellschaft zur Förderung der Wissenschaften e.V. digitalisiert und unter folgender Lizenz veröffentlicht: Creative Commons Namensnennung-Keine Bearbeitung 3.0 Deutschland Lizenz.

Zum 01.01.2015 ist eine Anpassung der Lizenzbedingungen (Entfall der Creative Commons Lizenzbedingung „Keine Bearbeitung“) beabsichtigt, um eine Nachnutzung auch im Rahmen zukünftiger wissenschaftlicher Nutzungsformen zu ermöglichen.

This work has been digitalized and published in 2013 by Verlag Zeitschrift für Naturforschung in cooperation with the Max Planck Society for the Advancement of Science under a Creative Commons Attribution-NoDerivs 3.0 Germany License.

On 01.01.2015 it is planned to change the License Conditions (the removal of the Creative Commons License condition "no derivative works"). This is to allow reuse in the area of future scientific usage.

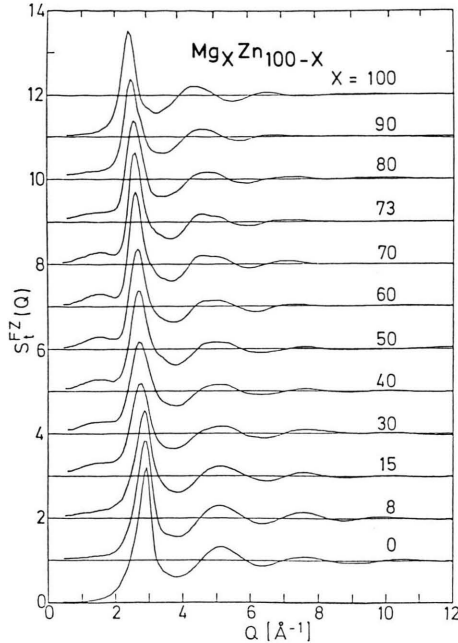


Fig. 1.  $\text{Mg}_x\text{Zn}_{(100-x)}$ -melts; X-ray diffraction (Mo-K $\alpha$ ); structure factors  $S_t^{FZ}(Q)$ ;  $T = T_L + 40^\circ\text{C}$ .

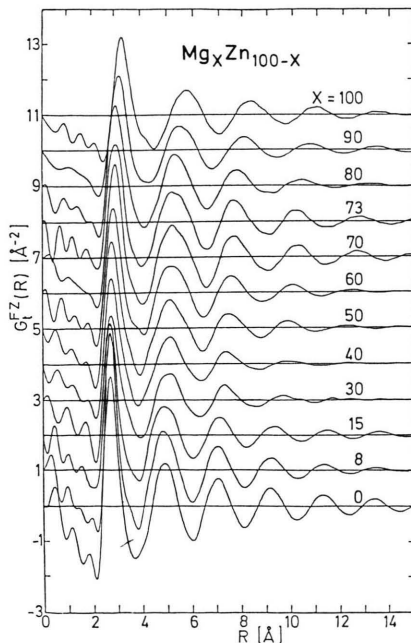


Fig. 2.  $\text{Mg}_x\text{Zn}_{(100-x)}$ -melts; X-ray diffraction (Mo-K $\alpha$ ); pair correlation functions  $G_t^{FZ}(R)$ ;  $T = T_L + 40^\circ\text{C}$ .

## 2. Total Pair Correlation Functions

Figure 2 shows the total pair correlation functions  $G_t^{FZ}(R)$  as obtained from the  $S_t^{FZ}(Q)$  in Fig. 1 by Fourier-transformation. The maxima shift to smaller  $R$ -values with increasing Zn-concentration. The oscillations are most pronounced for the two elements Mg and Zn. The strong oscillations in the  $\text{Mg}_{70}\text{Zn}_{30}$ - as well as the  $\text{Mg}_{73}\text{Zn}_{27}$ -curves also should be mentioned. The height of the main maximum for the concentrations  $100 \geq x \geq 30$  remains nearly unchanged but it increases for  $15 \geq x \geq 0$  by nearly 80%.

The coordination numbers were determined according to the minimum-minimum method. These coordination numbers for the first ( $N^I$ ) and second ( $N^{II}$ ) coordination spheres as well as the corresponding atomic distances  $R^I$  and  $R^{II}$  are presented in Table 1.

We note that from the concentration dependence of the  $R$ - and  $N$ -values in Table 1 a tendency for compound formation cannot be derived [11]. Thus, up to this point the only hints for compound formation within the  $\text{Mg}_x\text{Zn}_{(100-x)}$ -alloys are the premaxima as observed in Fig. 1, which will be treated in the following.

## 3. Short Range Order

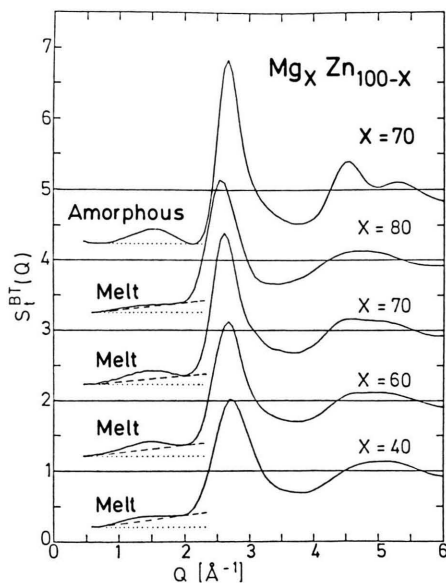
As mentioned above, the CSRO contributes to the structure factor in the region of  $0.5 \text{ Å}^{-1} \leq Q \leq 2 \text{ Å}^{-1}$  by forming a prepeak which is to be ascribed to the Bhatia Thornton partial structure factor  $S_{CC}(Q)$  [12], describing the correlations between

Table 1.  $\text{Mg}_x\text{Zn}_{100-x}$ -melts; coordination numbers and coordination radii.

Specimen	$N^I$	$N^{II}$	$R^I$ [Å]	$R^{II}$ [Å]
Mg	10.7	37.2	3.17	6.25
$\text{Mg}_{90}\text{Zn}_{10}$	10.7	37.6	3.06	6.00
$\text{Mg}_{80}\text{Zn}_{20}$	11.2	37.9	2.97	5.70
$\text{Mg}_{73}\text{Zn}_{27}$	11.1	37.9	2.93	5.70
$\text{Mg}_{70}\text{Zn}_{30}$	11.4	42.3	2.92	5.70
$\text{Mg}_{60}\text{Zn}_{40}$	11.7	38.2	2.83	5.60
$\text{Mg}_{50}\text{Zn}_{50}$	11.6	39.8	2.77	5.80
$\text{Mg}_{40}\text{Zn}_{60}$	11.2	29.5	2.75	5.35
$\text{Mg}_{30}\text{Zn}_{70}$	11.8	32.3	2.73	5.35
$\text{Mg}_{15}\text{Zn}_{85}$	11.3	36.1	2.70	5.30
$\text{Mg}_{08}\text{Zn}_{92}$	12.2	37.7	2.70	5.15
Zn	12.1	38.4	2.70	5.10

Table 2. Amorphous  $\text{Mg}_{70}\text{Zn}_{30}$  as well as those  $\text{Mg}_x\text{Zn}_{(100-x)}$ -melts which show a premaximum in the structure factors. Parameters for characterization of the short range order. $Q^P, Q^I$ : Position of prepeak and main maximum, respectively. $\Delta Q^P, \Delta Q^I$ : Width of those maxima. $I^P$ : Height of prepeak. $\xi^C, \xi^T$ : Correlation lengths of the chemical and topological short range order, respectively.

Specimen	$Q^P$ [Å <sup>-1</sup> ]	$Q^I$ [Å <sup>-1</sup> ]	$\Delta Q^P$ [Å <sup>-1</sup> ]	$\Delta Q^I$ [Å <sup>-1</sup> ]	$Q^P/Q^I$	$I^P$	$\xi^C$ [Å]	$\xi^T$ [Å]	$S_{CC}(Q^P)$
$\text{Mg}_{80}\text{Zn}_{20}$	1.55	2.59	—	0.44	0.60	0.02	—	14.2	0.15
$\text{Mg}_{73}\text{Zn}_{27}$	1.55	2.60	0.71	0.44	0.60	0.10	8.80	14.2	0.55
$\text{Mg}_{70}\text{Zn}_{30}$	1.52	2.60	0.70	0.44	0.58	0.11	8.80	14.2	0.58
$\text{Mg}_{60}\text{Zn}_{40}$	1.52	2.67	0.66	0.44	0.57	0.09	9.50	14.2	0.52
$\text{Mg}_{50}\text{Zn}_{50}$	1.50	2.72	0.66	0.51	0.55	0.08	9.50	12.3	0.52
$\text{Mg}_{40}\text{Zn}_{60}$	1.50	2.73	—	0.54	0.55	0.06	—	11.6	0.46
$\text{Mg}_{30}\text{Zn}_{70}$	1.50	2.75	—	0.52	0.54	0.04	—	—	0.40
$\text{Mg}_{70}\text{Zn}_{30}$ amorphous	1.54	2.65	0.78	0.44	0.58	0.27	8.10	14.2	1.48

Fig. 3.  $\text{Mg}_x\text{Zn}_{(100-x)}$ -melts; total Bhatia Thornton structure factors; upper curve: amorphous  $\text{Mg}_{70}\text{Zn}_{30}$ .

concentration fluctuations. To evaluate  $S_{CC}(Q)$  two further diffraction experiments are necessary or one further diffraction experiment in favourable cases where the contribution of  $S_{NC}(Q)$  can be neglected. Recently, with molten  $\text{Mg}_{72}\text{Zn}_{28}$  a neutron diffraction experiment was performed [10]. Since the corresponding data are not yet at our

disposal, in the present paper we discuss the X-ray results only.

The discussion starts from Bhatia Thornton total structure factors as shown in Figure 3. These functions yield data as given in Table 2.

$\Delta Q^P$  and  $\Delta Q^I$  are the widths of the prepeak and the main maximum, respectively. The correlation lengths were estimated according to the Scherrer formula [13]

$$\xi^{C,T} = 2\pi/\Delta Q^{P,I}. \quad (2)$$

$\xi^C$  follows from the width of the prepeak and amounts to about 8 Å for  $x \geq 50$  and up to 9 Å for  $x < 50$ .  $\xi^T$  decreases from 14 Å for  $x = 80$  down to 12 Å for  $x = 30$ . The amplitude of the prepeak  $I^P$  was estimated as shown in Fig. 3, namely as distance between the broken line and the maximum height of the prepeak.  $I^P$  is related to the partial structure factor  $S_{CC}(Q)$ , which is a measure for the CSRO according to

$$I^P = \frac{(f_A - f_B)^2}{(c_A f_A^2 + c_B f_B^2)} c_A c_B S_{CC}(Q^P) \quad (3)$$

with  $f_A, f_B$  = scattering length of species A, B,  
 $c_A, c_B$  = atomic fraction of species A, B.

Thus  $S_{CC}(Q^P)$  can be estimated, and according to Table 2 the strongest CSRO is observed for the

$\text{Mg}_{70}\text{Zn}_{30}$ -melt. In the  $\text{Mg}_{30}\text{Zn}_{70}$ -melt the CSRO amounts to 70% of that of the  $\text{Mg}_{70}\text{Zn}_{30}$ -melt, whereas it amounts to 26% in the case of  $\text{Mg}_{80}\text{Zn}_{20}$ . As can be seen in Fig. 3, the value of the CSRO depends on the choice of the broken line and thus is not well defined. The use of the dotted lines as in the case of amorphous  $\text{Mg}_{70}\text{Zn}_{30}$  [9] would yield larger values for the CSRO. According to [14] the influence of the CSRO-parameter  $\alpha^I$  of the first coordination shell on the so called short range order scattering  $I_{\text{CSRO}}$  can be written as

$$I_{\text{CSRO}} = c_A c_B (f_A - f_B)^2 N^I \alpha^I \frac{\sin(QR)^P}{(QR)^P}. \quad (4)$$

For compound forming systems,  $\alpha^I$  is negative and leads to the formation of the prepeak at  $Q^P R^P = 4.49$ . Thus from the  $Q^P$ -values of Table 2 we obtain  $R^P$  in the range 2.9 Å up to 3.0 Å.

The prepeak in  $S(Q)$  is most pronounced for the  $\text{Mg}_{70}\text{Zn}_{30}$ -melt from which easily the corresponding amorphous phase can be obtained by rapid quenching. But also for the  $\text{Mg}_{80}\text{Zn}_{20}$ - and the  $\text{Mg}_{30}\text{Zn}_{70}$ -melt a prepeak is observed. Since these melts cannot be frozen down to the amorphous state, the occurrence of a prepeak seems not to be uniquely characteristic for those alloy compositions which may lead to the formation of the amorphous state. The splitting up of the second peak in  $S(Q)$ , however, indicates the capability to produce the corresponding alloy in the amorphous form.

#### 4. Comparison of the Molten and the Amorphous State

For comparison with the results obtained with the  $\text{Mg}_{70}\text{Zn}_{30}$ -melt, an amorphous  $\text{Mg}_{70}\text{Zn}_{30}$ -alloy was

produced by melt spinning and investigated using the same arrangement as for the molten state. Furthermore the a- $\text{Mg}_{70}\text{Zn}_{30}$  was investigated after annealing for two hours at 90 °C. The comparison of the structure factors obtained with the molten, the amorphous, and the annealed  $\text{Mg}_{70}\text{Zn}_{30}$  specimen shows complete accordance with the results of [4] and [15]. Molten as well as amorphous  $\text{Mg}_{70}\text{Zn}_{30}$  shows a prepeak which is less pronounced in the molten case than for amorphous  $\text{Mg}_{70}\text{Zn}_{30}$ . The structure factor of the annealed specimen shows instead of the prepeak three isolated Bragg-peaks which correspond to those obtained in [16] for crystalline  $\text{Mg}_{51}\text{Zn}_{20}$  ( $c_{\text{Mg}} = 71.8$  a/o). From the observation that the total structure factor for molten, amorphous, and annealed  $\text{Mg}_{70}\text{Zn}_{30}$  shows a prepeak or Bragg-reflexions in the corresponding  $Q$ -region we deduce a similarity between the CSRO in the amorphous [10], the annealed, and the molten state. The correlation lengths  $\xi_{\text{melt}}^C = 8.8$  Å and  $\xi_{\text{amorphous}}^C = 8.1$  Å, as well as  $\xi_{\text{melt}}^T = 14.2$  Å and  $\xi_{\text{amorphous}}^T = 14.2$  Å are in good accordance.

Both the structure factors and the pair correlation functions show that the atomic arrangement in the molten state is not as well defined as in the corresponding amorphous state.

#### Acknowledgements

Thanks are due to the Deutsche Forschungsgemeinschaft for financial support.

- [1] S. Steeb and R. Hezel, *Z. Metallk.* **57**, 374 (1966).
- [2] S. Steeb and H. Entress, *Z. Metallk.* **57**, 803 (1966).
- [3] W. E. Lukens and C. N. J. Wagner, *Z. Naturforsch.* **28a**, 297 (1973).
- [4] H. Rudin, S. Jost, and H.-J. Güntherodt, *J. Non-Cryst. Solids* **61, 62**, 291 (1984).
- [5] K. Sagel, *Tabellen zur Röntgenstrukturanalyse*, Springer-Verlag, Berlin 1958.
- [6] G. Hermann, Doctor thesis, University of Stuttgart 1980.
- [7] J. Krogh-Moe, *Acta Cryst.* **9**, 951 (1956).
- [8] J. H. Hubbel, W. J. Veigle, E. A. Briggs, R. T. Brow, D. T. Cromer, and R. J. Howeston, *J. Phys. Chem. Ref. Data* **4**, 471 (1975).
- [9] E. Nassif, P. Lamparter, W. Sperl, and S. Steeb, *Z. Naturforsch.* **38a**, 142 (1983).
- [10] P. Andonov and P. Chieux, *J. Physique, Colloque* **C8-81**, 81 (1985).
- [11] E. Bühler, Doctor thesis, University of Stuttgart 1986.
- [12] A. Bhatia and D. E. Thornton, *Phys. Rev.* **B2**, 3004 (1970).
- [13] P. Scherrer, *Natur. Ges. Wiss. Göttingen* 1918, p. 98.
- [14] A. Boos, Doctor thesis, University of Stuttgart 1977.
- [15] M. Ito, H. Narumi, T. Mizoguchi, T. Kawamura, H. Iwasaki, and N. Shiotani, *J. Physical Soc. Japan* **54**, 1843 (1985).
- [16] I. Higashi, N. Shiotani, M. Uda, T. Mizoguchi, and H. Katoh, *J. Solid State Chem.* **36**, 225 (1981).